

PAPER • OPEN ACCESS

## Fabrication & Characterization of AlAs/pSi Heterojunction Solar Cell

To cite this article: Hanan K Hassun *et al* 2018 *J. Phys.: Conf. Ser.* **1003** 012110

View the [article online](#) for updates and enhancements.

### Related content

- [Calculations of bound states in the valence band of AlAs/GaAs/AlAs and AlGaAs/GaAs/AlGaAs quantum wells](#)  
S Brand and D T Hughes
- [Fabrication and characterization study of ZnTe/n-Si heterojunction solar cell application](#)  
BushraK H AlMaiyaly, Bushra H Hussein and Aday H Shaban
- [THE DOUBLE-LINED SPECTROSCOPIC BINARY PSI ORIONIS.](#)  
W. Lu

# Fabrication & Characterization of AIAS/pSi Heterojunction Solar Cell

Hanan K Hassun<sup>1</sup>, Auday H Shaban, Ebtisam M T Salman

Department of physics College of Education For Pure Science Ibn AlHaitham  
University of Baghdad Baghdad Iraq

hanan.kadhem@yahoo.com

**Abstract:** Silver Indium Aluminum Selenium  $\text{AgIn}_{1-x}\text{Al}_x\text{Se}_2$  AIAS for  $x=0.1$  thin films was deposited by thermal evaporation at RT and different thickness 100 150 and 200 nm on the glass Substrate and pSi wafer to produce AIAS/pSi heterojunction solar cell. Structural optical electrical and photovoltaic properties are investigated for the samples. XRD analysis reveals that all the deposited AIAS films show polycrystalline structure without any change due to increase of thickness. Average diameter and roughness calculated from AFM images shows an increase in its value with increasing thickness. The optical absorbance and transmittance for samples are measured using a spectrometer type UV Visible 1800 spectral photometer to study the energy gap. The electrical properties of heterojunction were obtained by IV dark and illuminated and C10V measurement. The ideality factor and the saturation current density were calculated. Under illuminated the open circuit voltage  $V_{oc}$  short circuit current density  $J_{sc}$  fill factor FF and quantum efficiencies were calculated. The built-in potential  $V_{bi}$  carrier concentration and depletion width are measured with different thickness.

**Keywords:** nAIAS/pSi heterojunction thin films solar cell

## 1. Introduction

The ternary chalcopyrite compounds of the group I–III–VI<sub>2</sub> direct gap semiconductors have been studied in recent years for solar cell applications due to their material properties as an absorbed layer for tandem solar cell light emitting diodes optoelectronics and nonlinear optical devices [1].  $\text{AgInSe}_2$  was first prepared from the original binary compounds by Hahnet et al [2].  $\text{AgInSe}_2$  thin films have been produced by several techniques such as coevaporation [3], ultrahigh vacuum pulsed laser deposition [5], horizontal Bridgman method [6], molecular beam epitaxial [7] and solid state microwave irradiation [8]. The growing and properties of AIGS thin films and devices fabricated with various film compositions are presented [9]. The aim of this study was focused on the fabrication and characterization of AIAS /pSi heterojunction for solar cells with different thin film thickness utilizing thermal evaporation technique.



## 2. Experimental

Polycrystalline AIAS material alloy was prepared by fusing the mixture of the appropriate quantities of the elements Ag In Al and Se of high purity 99999% in evacuating fused quartz ampoules The compound of  $\text{AgIn}_{1-x}\text{Al}_x\text{Se}_2$  were sealed in a quartz ampoule at a base pressure of  $10^3$  Torr The ampoule's temperature was raised from room temperature to 1200 K for five hour with a rate of 5 K/min in an electrical furnace The sample was left to cool slowly in the electrical furnace

The films of different thicknesses 100 150 and  $200 \pm 20$  nm were determined by using optical interferometer method and deposited by the thermal evaporation technique at room temperature using the Edward coating unit model E 306 of  $3 \times 10^6$  Torr using with molybdenum boat were prepared onto a glass slide substrate and single crystal pSi 111 The area of heterojunction solar cell was 1 cm Xray diffraction XRD was used in order to identify the structural of the deposited  $\text{AgIn}_{1-x}\text{Al}_x\text{Se}_2$  films The average crystallite size  $C_s$  of AIAS thin films was calculated by using Scherer's formula [10]

$$C_s = \frac{0.94\lambda}{B \cos \theta_B} \dots \dots \dots (1)$$

$\lambda$  = X ray wavelength  $\beta$  = full width at half maximum of the main peak and  $\theta$  = reflection angle

The surface morphology and roughness were studied by atomic force microscope AFM. The optical absorption spectrum of the prepared  $\text{AgIn}_{1-x}\text{Al}_x\text{Se}_2$  thin film will be considered through UV-VIS spectrophotometer at 25°C The energy gap  $E_g$  and the absorption coefficient were determined by equations [11 12]

$$\alpha h\nu = D h\nu - E_g^r \quad (2)$$

$$\alpha = 2303 A/t \quad (3)$$

Where  $\alpha$  is the absorption coefficient  $D$  is a constant dependent on the properties of the bands  $h\nu$  is the photon energy eV  $E_g$  is the optical energy gap eV  $r$  is constant and may take values 2 31/2 3/2 reliant on the material and the type of the optical transition  $A$  is the absorbance and  $t$  is the film thickness

Hall Effect measurements have been managed by Vander Pauw Ecopia HMS 3000 to determining majority carrier concentrations type of carrier and their mobility in thin films

IV characteristics of Al AIAS /pSi heterostructures in dark and under light were measured The Current – Voltage characteristics in illumination and dark is description by the equation respectively [13]

$$I = I_s \left( \exp\left(\frac{qV}{\beta K_B T}\right) - 1 \right) - I_L \dots \dots \dots (4)$$

The ideality factor can calculated from equation

$$\beta = \frac{q}{K_B T} \frac{dV}{d(\ln I)} \dots \dots \dots (5)$$

Where  $I_s$  Saturation current  $I_L$  Illumination current  $I$  The total current Solar cell current  $V$  applied voltage positive forward bias and negative for reverse bias  $T$  Temperature in Kelvin  $K_B$  Boltzmann constant  $q$  electron charge  $\beta$  is the ideality factor related to the many physical properties of the heterojunction having a value between 1 and 2

The photovoltaic conversion efficiency and Fill Factor is given by [13]

$$\eta = \frac{P_m}{P_{in}} \times 100\% = \frac{I_m V_m}{P_{in}} \times 100\% \dots \dots \dots (6)$$

$$F.F = \frac{J_m V_m}{J_{sc} V_{oc}} \quad (7)$$

The capacitance–voltage C–V distinguishing for nAIAS/pSi heterojunction was obtained through LCZ meter at frequency = 10 MHz. The capacitance voltage measurements led to calculate different factors for example built in potential junction capacitance charge carrier concentration and depletion region thickness from [14]

$$C = \left[ \frac{q \epsilon_n \epsilon_p N_n N_p}{2(\epsilon_n N_n + \epsilon_p N_p)} \right]^{1/2} (V_{bi} - V)^{-1/2} \quad \dots\dots\dots (8)$$

$N_n$  and  $N_p$  are the donor concentrations in nAgInAlSe<sub>2</sub> and the acceptor concentrations in pSi,  $\epsilon_n$  and  $\epsilon_p$  are the dielectric constants of nAgInAlSe<sub>2</sub> and pSi respectively,  $V_{bi}$  is the built in potential and  $V$  is the applied voltage

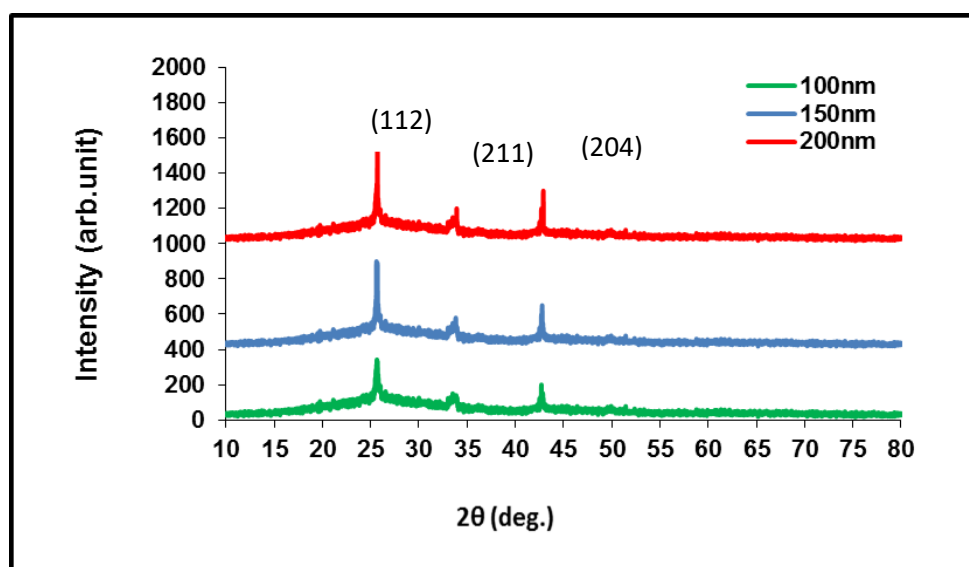
$$W = \frac{\epsilon_s}{C_0} \quad \dots\dots\dots (9)$$

$$\epsilon_s = \frac{\epsilon_n \epsilon_p}{\epsilon_n + \epsilon_p} \quad \dots\dots\dots (10)$$

Where  $W$  is the width of the depletion region,  $C_0$  is the capacitance at zero biasing voltage and  $\epsilon_s$  is the dielectric constant of heterojunction

### 3. Results and discussion

Figure 1 shows the XRD spectrum of different thickness 100, 150 and 200 ± 20 nm of AIAS thin films deposited on glass. The patterns show that all the films have three main crystalline peaks: the first peak located at  $2\theta \approx 25.18^\circ$  with the 112 preferred orientation, while the second peak appeared at  $2\theta \approx 33.5^\circ$  with the 211 and the third peak appeared at  $2\theta \approx 42.7^\circ$  with the 204. Table 1 shows all the peaks observed in all films. By increasing the film thickness, the locations of the measured diffraction peaks do not change significantly, but the intensities of the peaks increase. This is due to the improvement of crystallinity of the films, and crystallite size becomes larger from 1723 to 591 nm when increased the film thickness [15].

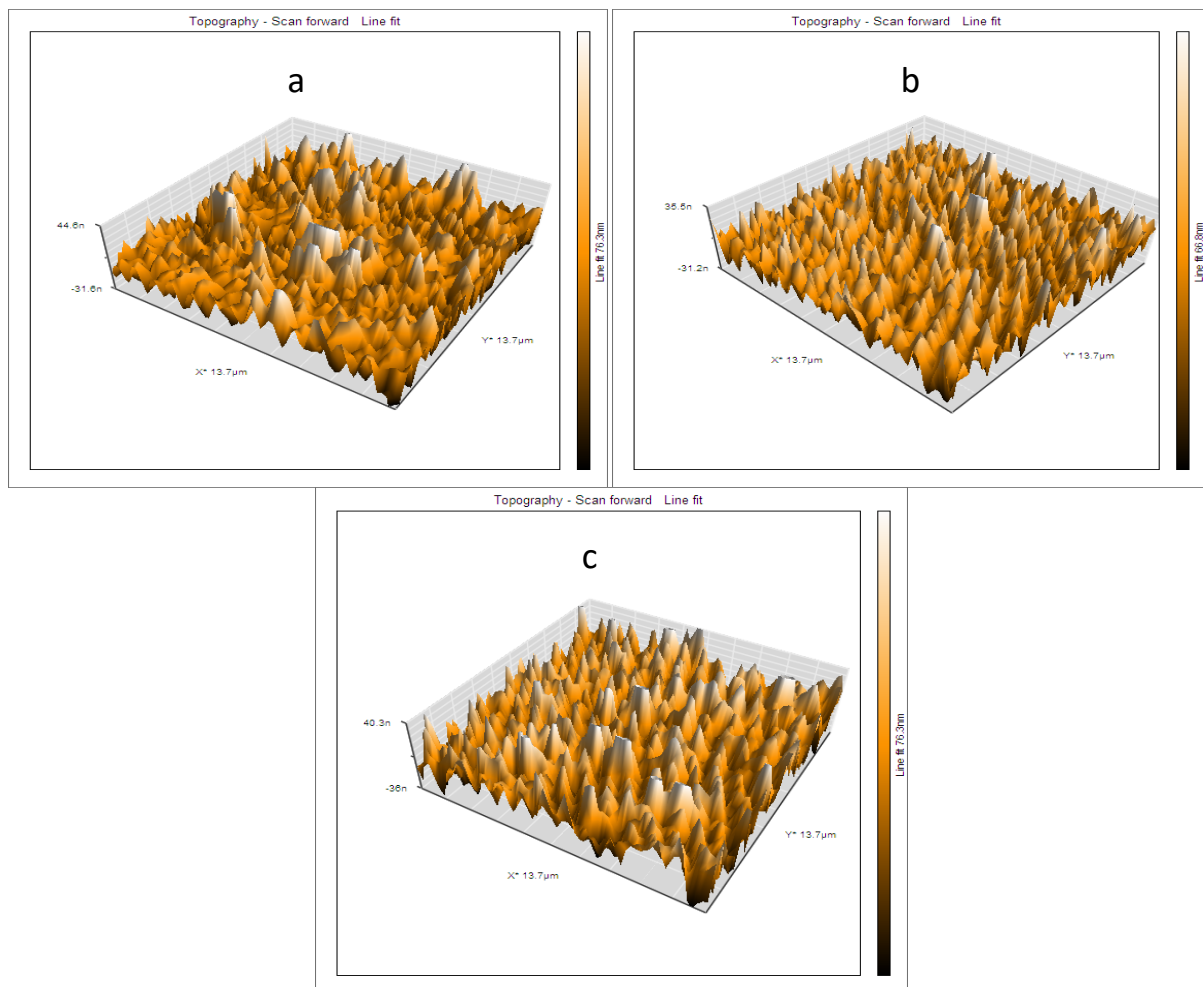


**Figure 1.** XRD patterns for AIAS thin films deposited on glass with different thicknesses 100, 150 and 200 nm

**Table 1.** Structural parameters of AIAS thin films at different thicknesses

Thicknessnm	2 $\theta$ Deg	d <sub>hkl</sub> ExpÅ	hkl	$\beta$ Deg	CSnm
100	2518	3532	112	04933	1723
	335	267	211		
	427	2115	204		
150	256	3475	112	0253	336
	3382	2647	211		
	4278	2111	204		
200	257	3462	112	0144	591
	3392	2639	211		
	429	2105	204		

'Figure 2' shows the AFM images of three dimensional 3D surface morphology of AIAS thin films with different thickness The surface roughness values and the grain size were measured and illustrated in table 2This is also supported by the Xray diffraction data The average diameter of AIAS thin films with respect to thickness seems to be larger in Figure 2 c than Figure 2 a 2b

**Figure 2.** 3D AFM images of AIAS with thicknesses a) 100 nm b) 150 nm and c) 200 nm

**Table 2** The average grain size GS and roughness for AIAS thin films at different thickness

Thicknessnm	Grain size GSnm	Roughness average nm	rmsnm
100	992	1278	1695
150	128	1424	1943
200	152	3843	6590

In order to probe the energy transitions within AIAS films the optical properties measurements were studied. The Absorbance and Transmittance spectrum of AIAS thin films was calculated as a function of wavelength at different thickness in figure 3. The Absorbance spectrum for AIAS thin film increase with the increase of thickness. The Absorbance values were between 40% and 85%. These results agree with other researchers [15].

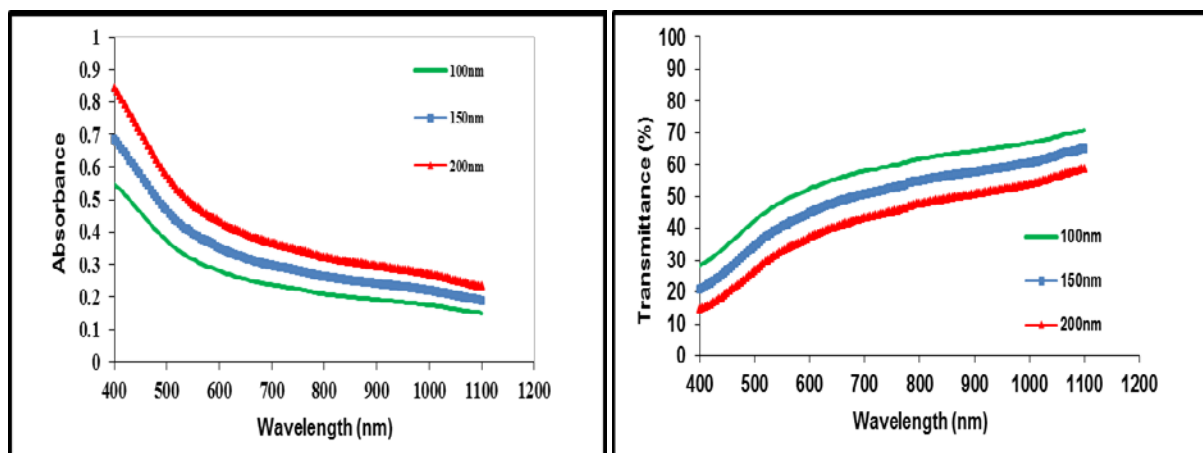


**Figure 3.** The Absorbance and Transmittance spectrum of AIAS with different thickness 100 nm 150 nm and 200 nm

The behavior of the transmittance spectra is opposite totally to that of the absorbance spectra. From Figure 4 we can observe that the  $\alpha$  values which has been calculated using equation 3 indeed own high amount reached above  $10^5 \text{ cm}^{-1}$ . It was pointed that the  $\alpha$  values in general increases as a function of different thickness which is attributed to an increase in absorbance of used films. We found that the value of  $\alpha$  increases from  $0.612 \times 10^5 \text{ cm}^{-1}$  with the increase of thickness. The value of  $E_g^{\text{opt}}$  decreases from 198 to 172 to 155 eV with increase of thickness as shown in figure 4. The decrease in the band gap  $E_g^{\text{opt}}$  values may be describable of the increase in defect states near the bands. This result is in agreement with reference [4].

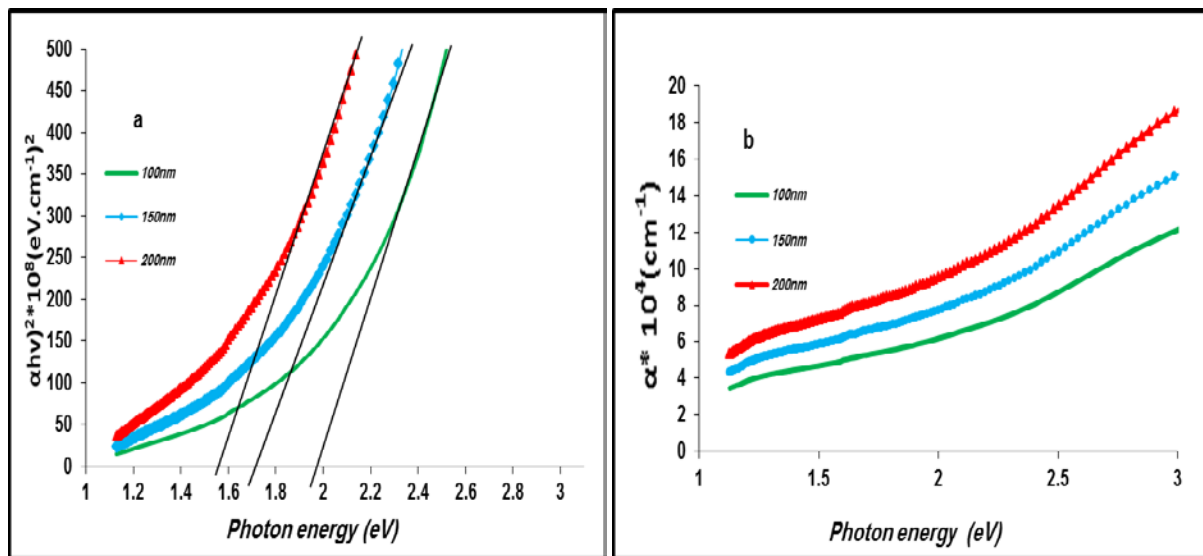


**Figure 4.** **a** Variation  $\alpha hv^2$  verse photon energy **b** absorption coefficient verse photon energy of AIAS with different thickness 100 nm 150 nm and 200 nm

The type of charge carriers concentration  $n$  and Hall mobility  $\mu_H$  has been estimated from Hall measurements. These values are listed in table 3. The negative sign of the Hall coefficient indicates that the conductive nature of the film is n-type. Electrons are the majority charge carriers, i.e., Hall voltage decreases with the increasing of the current. The carrier concentration of the order  $10^{16} \text{cm}^{-3}$  is in a good agreement with reference [16]. We can notice from table 3 that the carrier concentration and mobility increases with increasing of thickness.

**Table 3** Hall parameters for AIAS thin films at different thickness

Thickness nm	$R_H$	$\mu_H \text{cm}^2/\text{VS}$	$n \text{cm}^{-3}$	$\rho \Omega \text{cm}$
100	8928571	7440476	7E+16	12
150	753012	125502	83E+16	6
200	6416838	1604209	974E+16	4

'Figure 5' illustrated IV curve of manufactured AIAS/Si heterojunction solar cells with different thickness 100, 150 and 200  $\pm 20$  nm at RT. Using equations 6, 7 was the conversion efficiency and Fill Factor calculation as shown in figure 5 and table 4. The photo current produced by the 100  $\text{mW}/\text{cm}^2$  white lamp, the results obtained where there is a clear increase in the value of the open circuit voltage  $V_{oc}$  and the value of short circuit current density  $J_{sc}$  maximum for both the current and the voltage value  $V_m J_m$  and the value of efficiency solar cell in terms of efficiency increases in general with increasing thickness and this goes back as we have already improved the increase the surface roughness, the absorption coefficient and charge carriers. This result agrees with [17].

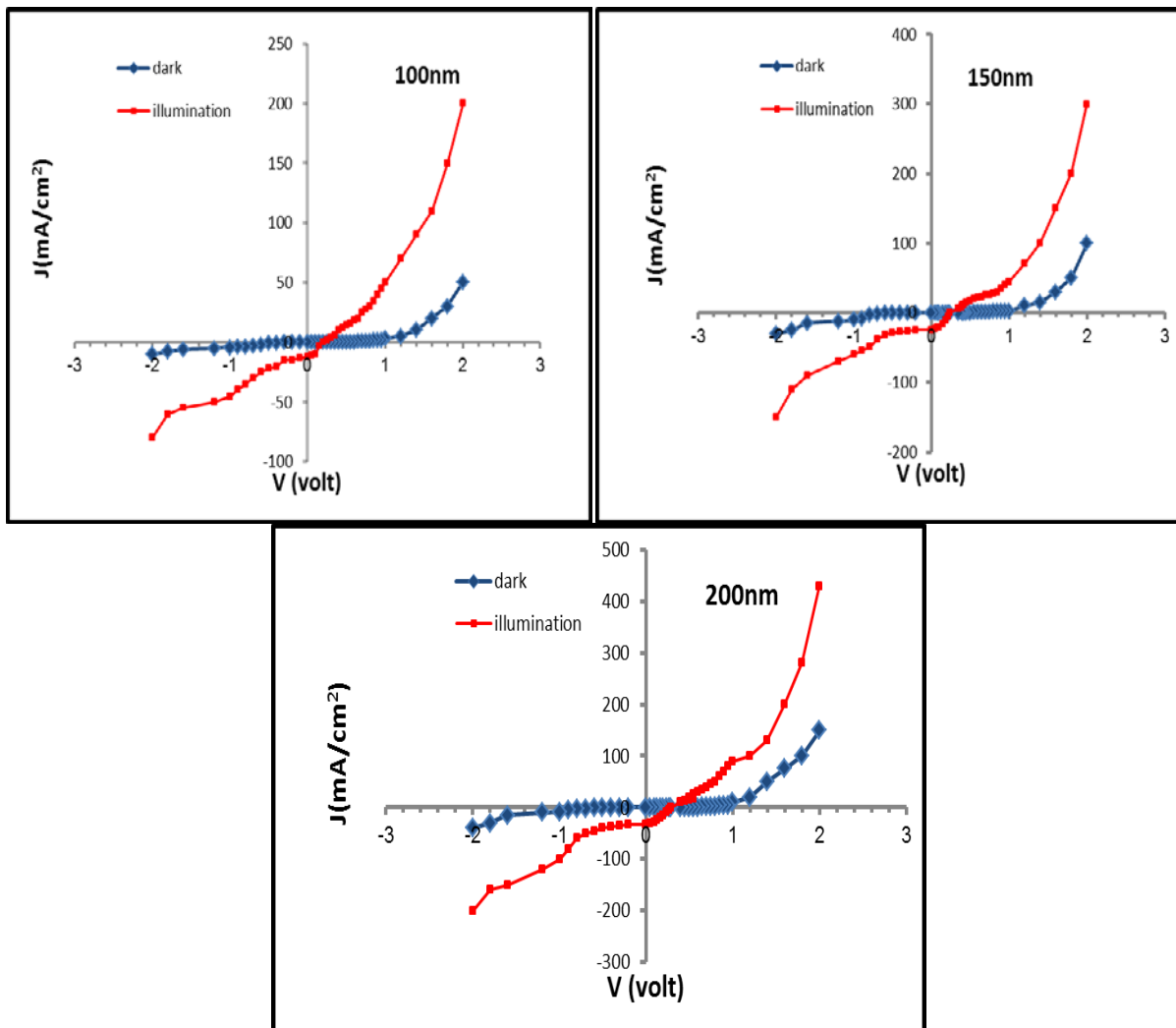


**Figure 5.** IV plots for AIAS/Si solar cell at thickness 100 150 200 nm in dark and under light

**Table 4.** The parameter for AIAS/Si heterojunction with respect to thicknesses

Thickness nm	$V_{oc}$ Volt	$J_{sc}$ $\text{mA}/\text{cm}^2$	$V_{max}$ Volt	$J_{max}$ $\text{mA}/\text{cm}^2$	FF	$\eta$ %
100	02	12	01	10	0416667	1
150	024	25	015	17	0425	255
200	029	32	017	20	0366379	34

The ideality factor  $\Phi_b$  and  $J_s$  of the AgInAlSe<sub>2</sub>/Si heterojunction solar cell are gained from the grade of the straight line region forward bias in IV plots under dark by using equation 5 as show in figure 6 and Table 5 the behavior of the current are change exponentially with voltage at  $V < 0.2$  V The decrease of ideality factor and  $\Phi_b$  with the increasing of thickness while  $J_s$  increase This result agrees with [18]



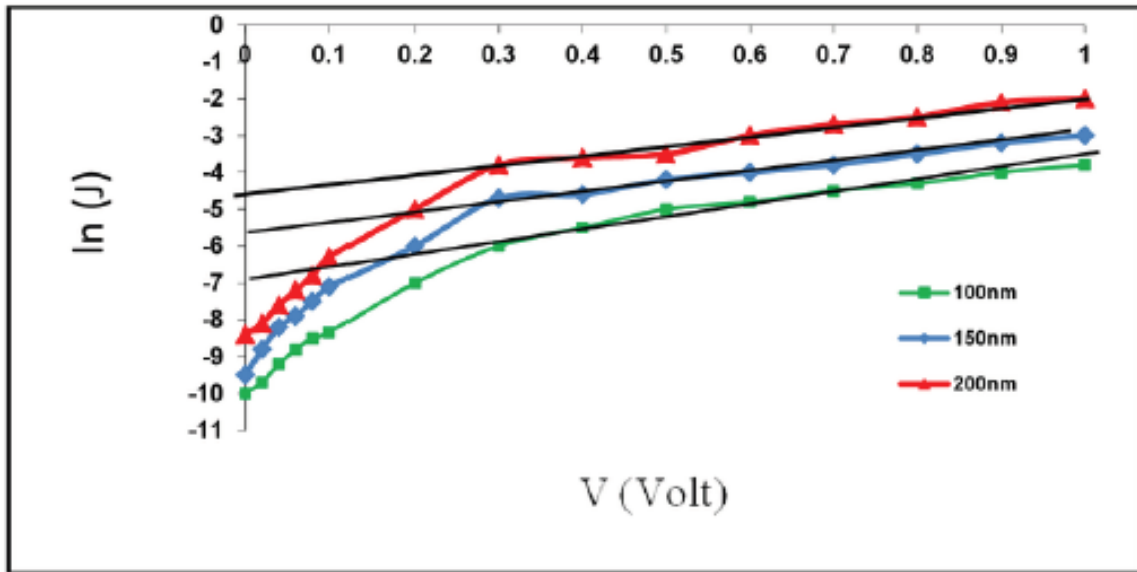


**Figure 6** ln J with V for forward bias for AIAS/Si junction in dark with respect to thicknesses

**Table 5.** Ideality Factor and  $J_s$  for AIAS /Si junction at different thicknesses

Thickness*nm	Ideality Factor	Saturation Current Density $J_s$ mA/cm <sup>2</sup>	Barrier*Height $\Phi_b$ eV
100	2193752	0000911882	060075
150	18263971	0003345965	056708
200	1668541	0008229747	054377

The capacitance voltage measurements led to calculate built in potential junction capacitance carrier concentration and depletion width Figure 7 illustrated  $1/C^2$  relation with respect to thickness amount For all samples it can be seen that junction capacitance is decrease with increasing bias voltage which can be explained by the expansion of depletion layer with the built in potential

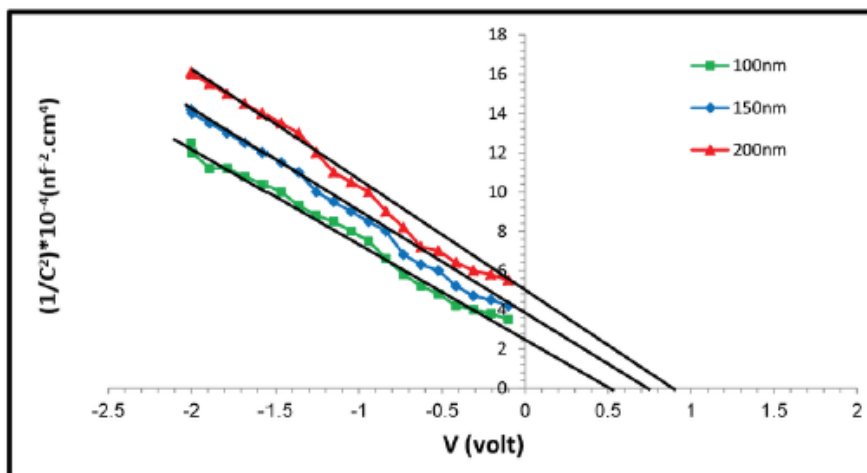


**Figure 7.**  $1/C^2$  as a function of reverse bias voltage for AIAS/Si heterojunction

Figure 7 illustrated CV behavior of AIAS/Si solar cell Table 6 illustrated the relation between  $C_0$  and thickness which is reversely relative This behavior was attributed to the increase in  $W$  which tends to the improve  $V_{bi}$  The increasing of  $W$  due to increases in thickness because of the increasing in  $N_D$  which leads to a decrease of the capacitance The CV measurements show that the heterojunction of abrupt type because the relationship between inverted square amplitude  $1/C^2$  with a voltage voltage of reverse bias is lined

**Table 6.** Variables of AIAS /Si heterojunction with different thickness

Thicknessnm	$C_0$ nf/cm <sup>2</sup>	$W=\epsilon_s/C_0$ nm	$V_{bi}$ Volt	$N_D$ cm <sup>3</sup>
100	6454972244	669	05	523001E+15
150	50	783	075	633278E+15
200	4472135955	876	09	77731E+15

#### 4. Conclusions

After characterizing and analyzing the performance of the samples the conclusions are summarized as follows

The AIAS thin films were successfully deposited on glass and silicon substrates by thermal evaporation technique The XRD analysis shows that all the deposited films were polycrystalline and the crystallite size was highly oriented in 112 direction AIAS films exhibits a high value of absorption coefficient in the visible range of the electromagnetic spectrum the optical transitions in AIAS are direct and value of optical energy gap decreases with increasing of thickness  $IV$  measurements analyzed minutely for rectifying and photovoltaic behaviors For AIAS/Si heterojunction solar cell the ideality factor and  $J_s$  are obtained with respect to different thickness The diode exhibits an ideal behavior when the ideality factors become less than 2 The measurements were carried out under illuminate by incident power density equal to about 100 mW/cm<sup>2</sup> The forward relativity between quantum and thickness will get the maximum values of efficiency 34 when the thickness  $t = 200$ nm while CV curves showed that the abrupt type for prepared devices

#### References

- [1] M Kaleli T Colakoglu M Parlak 2013 Production and characterization of layer by layer sputtered singlephase AgInSe<sub>2</sub>thin film by thermal selenization *Applied Surface Science* **286** 171 176
- [2] H Hahn G Frank W Klingler AD Meyer G 1952 StöergerTernareChalkogenideZeitschrift fur AnorganischeChemie 271 153 170
- [3] MC Santhosh Kumar and B Pradeep 2009 Effect of H<sup>+</sup> irradiation on the optical properties of vacuum evaporated AgInSe<sub>2</sub>thin films *Appl Surf Sci***255** 8324 8327
- [4] JJ Lee JD Lee BY Ahn HS Kim KH Kim 2007 Structural and Optical Properties of AgInSe<sub>2</sub> Films Prepared on Indium Tin Oxide Substrates *J KorPhysSoc***50** 1099 1103
- [5] H Mustafa D Hunter AK Pradhan UN Roy Y Cui A Burger Synthesis and characterization of AgInSe<sub>2</sub> for application in thin film solar cells *Thin Solid Films***515** 7001 7004
- [6] IV Bodnar 2004 Properties of AgGa<sub>x</sub>In<sub>1-x</sub>Se<sub>2</sub> Solid Solutions *Inorg Mater* 40 914918
- [7] K Yamada N Hoshino T Nakada 2006 Crystallographic and electrical properties of wide gap Ag In<sub>1-x</sub>Ga<sub>x</sub> Se<sub>2</sub>thin films and solar cells *SciTechnolAdv Mater***7** 4245
- [8] JW Lekse AM Pischera JA Aitken 2007 Understanding solidstate microwave synthesis using the diamondlike semiconductor AgInSe<sub>2</sub> as a case study *Mater Res Bull* **42** 395403
- [9] Keiichirou Yamada Nobuyuki Hoshino TokioNakada 2006 Crystallographic and electrical properties of wide gap Ag In<sub>1-x</sub>Ga<sub>x</sub> Se<sub>2</sub> thin films and solar cells *Science and Technology of Advanced Materials***7** 42 45
- [10] BD Cullity 1978 Elements of XRay diffraction 2nd edition copyright © by Addison Wesley

Publishing company *Inc*

- [11] Rutuparna Mohanty 2012 Electronic Properties of Ternary and Binary Compounds Thesis Submitted for the Award of the Degree of Master of Science Department of Physics National Institute of Technology
- [12] MA Omer 1975 Elementary Solid State *Physics Addison Wesley Publishing*
- [13] D A Neamen 2003 Semiconductors physics and Devices Basic Principles Third edition copyright© McGraw Hill Companies *Inc*
- [14] S M Sze 2007 Physics of semiconductors Devices Third edition copyright© by John Wiley & Sons *Inc*
- [15] S Murugana and KR Murali 2014 Structural Optical and Electrical Studies on Pulse Plated AgInSe<sub>2</sub> Films *ACTA PHYSICA POLONICA A* **126** 3 727731
- [16] Kenji Yoshino Aya Kinoshita Yasuhiro Shirahata Minoru Oshima Keita Nomoto Tsuyoshi Yoshitake Shunji Ozaki Tetsuo Ikari 2008 Structural and electrical characterization of AgInSe<sub>2</sub> crystals grown by hotpress method *Journal of Physics Conference Series* **14**
- [17] Raviendra D JK 1985 Sharma nCdS pAgInSe<sub>2</sub> solar cells by electro deposition physics status solidi *Application and materials science* **88** 1 365368
- [18] S Mridha M Dutta Durga 2009 Basak Photo response of nZnO/pSi heterojunction towards ultraviolet visible lights thickness dependent behavior *J Mater Sci Mater Electron* **20** 376